

Supplemental Data

Mammalian BTBD12/SLX4 Assembles

A Holliday Junction Resolvase

and Is Required for DNA Repair

Jennifer M. Svendsen, Agata Smogorzewska, Mathew E. Sowa, Brenda C. O'Connell, Steven P. Gygi, Stephen J. Elledge, and J. Wade Harper

Supplemental Experimental Procedures

Cell culture and plasmids

U2OS, DR-U2OS, HeLa, and 293T were grown in Dulbecco Modified Eagle medium (DMEM) supplemented with 10% (v/v) FBS (Invitrogen). In some cases, cells were cultured in media containing 100 units of penicillin per ml, and 0.1 mg streptomycin per ml.

Plasmids were constructed using recombinational cloning via the Gateway system (Invitrogen, Inc). Open reading frames in either pDONR or pENTR derivatives were recombined into the appropriate recipient vector using λ recombinase. The sources of open reading frames and primers used for PCR are shown in Table S2. All open reading frames were sequence validated.

Mass spectrometry and protein interaction

The methodology employed for mass spectrometry and data analysis is described in Sowa et al (Sowa, 2009). Briefly, the indicated proteins were expressed in 293T cells using either an MSCV-based LTR driven retrovirus (N-terminal HA-FLAG tag) or a CMV driven lenti-virus (pHAGE vectors kindly provided by Alex Balazs and Richard Mulligan, Harvard Medical School) (N/C-terminal HA-FLAG tag, Tet inducible C-HA). Cells expressing these proteins were lysed in lysis buffer (50 mM Tris-HCl pH 7.5, 150 mM NaCl, 0.5% Nonidet P40, 1mM EDTA) + protease inhibitors (ROCHE), and phosphatase inhibitors (10mM NaF, 10mM NPP, 10mM β -glycerophosphate, 0.1 μ M okadaic acid) and cleared lysates were subjected to immunoprecipitation using anti-HA antibodies covalently coupled to agarose beads. After 5 washes, beads were exchanged into PBS and proteins were eluted with synthetic HA peptide. The HA peptide was removed by precipitation of the proteins using trichloroacetic acid (20%, followed by a 10% TCA wash and 3 100% Acetone washes). Proteins were trypsinized and processed for mass spectrometry (LC-MS/MS) on an LTQ ion trap instrument as described previously (Sowa, 2009). Mass spectrometry data was processed using the comparative proteomics analysis software suite *CompPASS* (Sowa, 2009) which uses total spectral counts (TSC) for each identified protein to determine D^N-scores and Z-scores using parallel data from 75 unrelated baits as a comparative analysis tool (the Dub dataset from (Sowa, 2009)). In plots of D^N-score versus Z-score, proteins with D^N-scores greater than 1 are considered to be high confidence candidate interacting proteins (HCIPs). The entire data sets for proteins identified by mass spectrometry are provided in Table S1.

For immunoprecipitation of endogenous proteins, cells were lysed in lysis buffer . Protein extract (1-2 mg) was pre-cleared with Protein A sepharose CL-4B (GE Healthcare) for 1 hour at 4° C. The supernatant was subsequently incubated at 4° C with α -SLX4^C (5 μ g) or a control rabbit antibody and Protein A sepharose CL-4B overnight. In control experiments, 15 μ g of antigenic peptide was added together with 5 μ g of anti-SLX4^C to the immunoprecipitation reaction. Following five washes in lysis buffer, the immunoprecipitates were eluted in SDS Laemli buffer and size-fractionated on a Tris-Acetate or Bis-Tris gels (Invitrogen) prior to blotting with the indicated antibodies. Endogenous IPs for ERCC4 and TERF2IP were performed as described above using α -ERCC4F (1 μ g) or α - TERF2IP (2 μ g) antibodies and proteins were separated on Tris-Glycine gels (Invitrogen).

For protein interaction studies, the indicated proteins were expressed in 293T cells and after 24-48 h, cells were lysed in lysis buffer, and cleared lysates used for immunoprecipitation with the indicated antibodies. Immune complexes were washed 4-5x with lysis buffer, resuspended in SDS laemli buffer and were subjected to polyacrylamide gel separation and immunoblotting with the indicated antibodies.

Two-hybrid analysis was performed as described (Xu et al., 2008).

Antibodies

Antibodies directed against SLX4 (α -SLX4^C) were generated in rabbits using a synthetic peptide (TRREKLQGRRRQPR) derived from the C-terminus (residues 1813-1826) and were affinity purified using immobilized antigenic peptide. An additional anti-SLX4 antibody made in mice (α -SLX4^M) was purchased from Novus (H00084464-B01). All other antibodies were from commercial sources: TERF2IP (Rap1), Bethyl (A300-306A); PLK1, Santa Cruz (F-8); MSH2, Abcam (ab52266); MUS81, Abcam (ab14387); ERCC4 (XP F), Thermo (clone 219); γ H2AX, Millipore (JBW301); TRF2, Millipore (4A794).

RNAi

Retroviral infections were done in the presence of 8 μ g of polybrene per ml of viral supernatant. Sequences of shRNAs expressed from pSMP are provided in Table S2. shRNAs were obtained from Open Biosystems. RNAimax (Invitrogen) was used for reverse siRNA transfections (25 nM in U2OS, 36 nM in HeLa) according to manufacturer's instructions. siRNAs were from Dharmacon and the sequences are provided in Table S2.

Multicolor competition assay

GFP-U2OS and dsRed-U2OS cells used in the assay were described previously (Smogorzewska et al., 2007). dsRed-U2OS cells were infected with a control shRNA and the GFP-U2OS cells were infected with experimental shRNAs. Seven to ten days later, red and green cells were counted, mixed 1:1 and plated in 12 well plates. One day following mixing, cells were treated with the indicated DNA damaging agent and cultured for 10-12 days with an appropriate split at day 5 of treatment. The ratios of green to red cells were assessed using the high throughput sampler on an LSRII analyzer (BD Biosciences). Experiments were done in triplicate and error bars represent standard deviations of the normalized levels of resistance. The resistance of GFP-U2OS cells infected with control shRNA was set to 100%.

HeLa and GFP-HeLa were used in siRNA based multicolor competition assays. HeLa and GFP-HeLa were reverse transfected with control siRNA or experimental siRNAs, respectively. 3 days later, no color and GFP cells were counted, mixed 1:1 and plated in 24 well plates. One day after mixing cells were treated with the indicated DNA damaging agent. Camptothecin treated cells were then maintained in drug for the duration of the experiment. Cells were cultured for 6-7 days and split when needed. Cells were analyzed as described above.

In vitro DNA cleavage assays

DNA cleavage assays were performed using 5'-³²P-end-labeled DNA substrates. Substrates were generated by annealing oligonucleotides and were purified by poly-acrylamide gel electrophoresis as described previously (Ciccia et al., 2003; Ip et al., 2008; Rass and West, 2006). The sequences employed are provided in Table S2. XO-OE refers to a static junction with 3' overhangs of 1 or 2 nucleotides while XO-BE refers to static holiday junctions with blunt ends (Figure S10). Radiolabeled substrates were incubated with the indicated immune complexes isolated in lysis buffer + 1mM DTT from the indicated cell lines as described above. Immune complexes were washed 3x in cleavage buffer (50 mM Tris pH 8.0, 5 mM MgCl₂, 40 mM NaCl, 1 mM DTT, 100 μ g/ml BSA) prior to addition of substrate. After 30 min at 37°C, reaction mixtures were treated with 1% proteinases K in SDS prior to electrophoresis on either 8% polyacrylamide gels (native) or 12% polyacrylamide-urea gels (denaturing). Reaction products were visualized by autoradiography. To examine cleavage symmetry, products were incubated with 400 units of T4 DNA ligase (1 h) prior to electrophoresis on denaturing gels (Ip et al., 2008).

Homologous Recombination (HR) Assay

HR assays were performed as described (Smogorzewska et al., 2007) (Xia et al., 2006). I-Scel was

delivered using adenovirus AdNGUS24i (kindly provided by Frank Graham and Philip Ng, McMaster University) with a multiplicity of infection of 10. Experiments were done in triplicate and error bars represent standard deviations of the normalized levels of HR. Relative HR of cells infected with control shRNA was set to 100%.

Generation of DSB damage

Microirradiation was performed as described previously (Bekker-Jensen et al., 2006). Cells were pre-treated with 10 μ M BrdU for 24 hours to sensitize them to the UVA laser. Cells were microirradiated using PALM MicroBeam with fluorescence illumination (Zeiss). The power of the 355 nM laser was set between 40-45%, which resulted in localized damage as judged by γ -H2AX staining. DAPI staining was intact under these conditions. Cells (HT1080 or U2OS as indicated) were fixed 30 min or 1 hour after irradiation and stained with DAPI. GFP-fusion proteins were visualized directly. For co-localization experiments, antibodies against γ -H2AX were used in indirect immunofluorescence staining.

Immunofluorescence staining

Immunofluorescence was performed as described in (Smogorzewska et al., 2007). Cells grown on autoclaved cover slips were rinsed in PBS and were fixed in 3.7% (w/v) formaldehyde (Sigma) diluted in PBS for 10 minutes at room temperature. Cells were washed once with PBS, permeabilized in 0.5% (v/v) NP40 in PBS for 10 minutes, washed again in PBS, and blocked with PBG (0.2% [w/v] cold fish gelatin, 0.5% [w/v] BSA in PBS) for 20 minutes. Coverslips were incubated with a primary antibody for 2 hours at room temperature or overnight at 4° C. After three 5-minutes washes with PBG, the coverslips were incubated with the appropriate secondary antibody. After three additional washes in PBG, the coverslips were embedded in Vectashield (Vector Laboratories) supplemented with DAPI. Triton pre-extraction was performed by incubating cells for 5 minutes at room temperature with 0.5% Triton in PBS. Cells were fixed and processed as above. Images were captured using a confocal microscope (Olympus). Any co-staining experiments included proper controls to exclude crossing of signal between channels.

Bacterial Purification of SLX1/SLX4-C and MUS81/EME1

For production of GST-SLX1 and His₆-SLX4-C in bacteria, open reading frames for the two proteins were recombined into pET-60 (GST, Amp^r) or pColA (His₆, Kan^r) vectors and genes co-expressed in BL21 (Rosetta) cells. Cells were lysed in lysis buffer containing protease inhibitors, sonicated 2x and cleared by centrifugation. Supernatants were purified with GSH-sepharose for 2hr and washed 5 times with lysis buffer. Buffer was then exchanged to TRIS buffer (50 mM Tris pH 7.5, 10% glycerol, 0.01% NP40) containing 0.1M NaCl, 1 mM DTT and complexes were eluted with 20 mM glutathione. Eluates were combined and purified with Nickel-NTA agarose as described by Ciccia et al, 2003. GST-SLX1^{E82A}/His SLX4C and GST-MUS81/His-EME1 (expression vectors kindly provided by S. West, Ciccia et al., 2003) complexes were prepared similarly. GST-SLX1 was prepared similarly but with a single GSH-Sepharose purification step.

Figure S1. Characterization of SLX4 antibodies. Extracts from 293T cells were immunoprecipitated using anti-SLX4^C antibodies in the presence and absence of competing antigenic peptide and washed immune complexes subjected to SDS-PAGE using anti-SLX4^M or anti-ERCC4 antibodies. The asterisk indicates apparent SLX4 breakdown products.

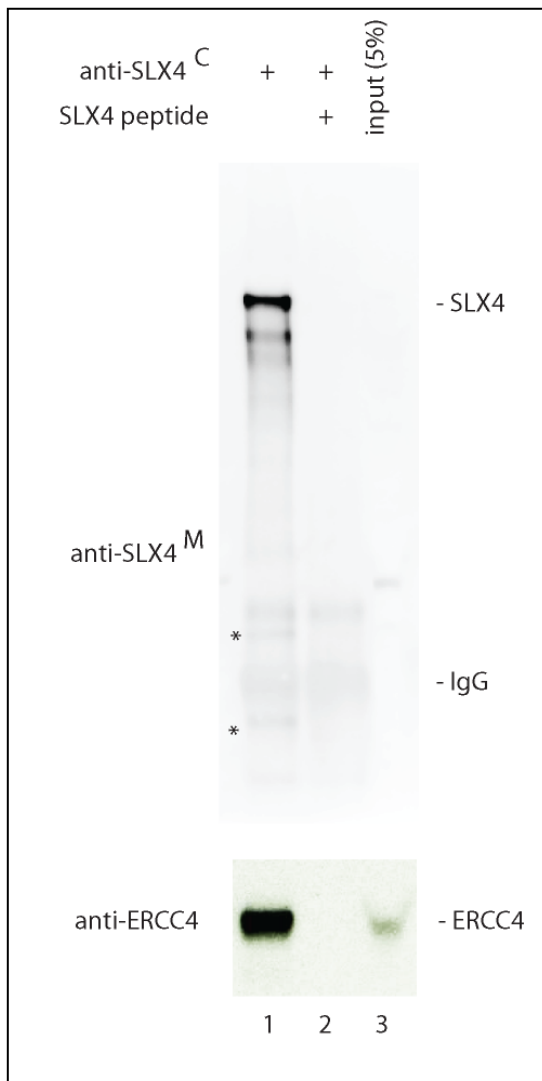


Figure S2. Multi-sequence alignments of eukaryotic SLX4/BTBD12-related proteins. Sequences were analyzed using CLUSTALW and displayed using BOXSHADE.

Figure S2 Continued

Figure S3. Multi-sequence alignments of eukaryotic SLX1-related proteins. Sequences were analyzed using CLUSTALW and displayed using BOXSHADE. Amino acid indicated with the asterisk (E82) is mutated to alanine in a inactive form of SLX1 used in this study.

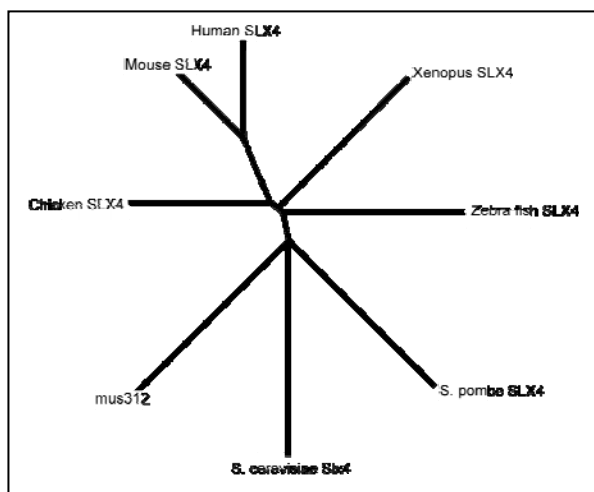
humanSLX1	1	-----	
mouseSLX1	1	-----	
frogSLX1	1	-----	
fishSLX1	1	-----	
flySLX1	1	-----	
wormSLX1	1	METFILSSDDDSGPPPSKRRRTIEGIPRSFSGDKKIRFSFGASNMSQDTTQEIIIPEDTDVTPLTIPSTPALSGKFDSKT	
pombeSLX1	1	-----	
Slx1p	1	-----	
consensus	1	-----	
humanSLX1	1	-----M	
mouseSLX1	1	-----	
frogSLX1	1	-----	
fishSLX1	1	-----	
flySLX1	1	-----LETNCINPYVGEFTDPQDTASE	
wormSLX1	81	PKSVRRRSVSMSCFTPIVETINQPPTNACSSFLQKEYNFHDLSDEGGDGGAGCSKDDEDKIIEDNLNLRLALLSPEKKK	
pombeSLX1	1	-----	
Slx1p	1	-----M	
consensus	81	-----	
humanSLX1	2	GPAGVAARPGRFVGYLLCL--NPYRGRIVYGFTVNNTARRVQHNGGRKGGAWRITSGRG--PWEMVLVHGFFSSVA	
mouseSLX1	1	--MDHARAPGRFVGYLLCQ--NPYRGRIVYGFTVNPARVRQHNAGRKGGAWRITSGRG--PWDMVLIHGFFSSAVA	
frogSLX1	1	--VVEVECYGVYLLCT--NPKYNGRIVYIGFTVNPERRIQHNGKHKGGAWRITSGRG--PWDMVLIHGFFNDIA	
fishSLX1	1	--MVVEVESFYGVYMLCT--NPKFNGRIVYIGFTVNPERRIQHNGRHRGGAKRTSGRG--PWDMVLIHGFFSDIA	
flySLX1	23	QQEETVALKGHFGVYLLCSQSLDPRFRKIVYGFTVNPKRRIROHNLCCDFGGAWRITSGRG--PWLVMVIVHGFFNNTV	
wormSLX1	161	RKEKDEVQNEFYGVICLRSRDRPCYLNRYIGNTVDPNRIMQHNGGRDGKAATDSRG--PWDMVIVVHGFFNNVVA	
pombeSLX1	1	--MDLCNFVCCYLLKSN--RTQSSAIVGSTPDPPRRLRQHN-CELVGAGSATKHGR--PWSISCLVYGFENKVVS	
Slx1p	2	SQKIQHQFFDFYCCVLEQSIN---KQSYFVSEIPNPVERRRLRHNGKLAVGGAERTKRDGSRPWEMLIVRGFFSKIA	
consensus	161	v FygvYlly npryrgrvYvGfTvnp RrqrQHnggrkGGAwrtsgrg PwemvlvhGFP va *	
humanSLX1	78	ALRFEWAQWHASRRLA---VGPBLIGEIAFAEHLRVLIAHMLRAPPWELPLTIRWVPDILQLCL----PPEPH	
mouseSLX1	75	ALRFEWAQWHQASRRLA---VGPBLIGEIAFAEHLRVLIAHMLRVPWPWPLTIRWLQDPLRHLCP----APPAH	
frogSLX1	73	ALRFEWAQWHHSRRLA---VPKTKHQSSFDHHLVLCMLRVPWPWPLTIRWLQDPLRHLCP----LQPPDH	
fishSLX1	73	ALRFEWAQWHHSRRLA---VPKTKHQSSFDHHLVLCMLRVPWPWPLTIRWLQDPLRHLCP----LQPPDH	
flySLX1	101	ALQFEAWQCPSESTRLKMPYERKRLPREFFDWNRFLSHMLGVCPWNLPLSVRWEETDYEERENM----PLPH	
wormSLX1	239	ALRFEAWQNPVSKSLKE--KQIQRERKEIIFPAQOLRHAECLMNSSAHCRFALITFRWLITTEELPPTS--CVPPH	
pombeSLX1	70	ALRFEAWQNLCISRYTKD--CDPFSMKQKTIIMCLGLPHLVDSDTWERWPLNITEINKTAFSEKINOL---GKTYGN	
Slx1p	78	ALQFEAWQHGYQHYAEKDRVWIKAGGRTLHHKAQMLLKLHEFFFORMLIIEVFNIKAWEVWKQDKFFIERDRFP	
consensus	241	ALrFEawQhp vsrrl h v rr rket f fhrlvl hmlrv p Rlpltrwl r dfr df pp h	
humanSLX1	149	VPIAFGPPPPQAPAP-----RAGPFDIAEPEPDQGDPGACSCCAQTQDEGP-----	
mouseSLX1	146	MPIAFGPPPPQPLVP-----RPAVSIAASERQLDLG-TKAACSLCPLRLQDPEGP-----	
frogSLX1	146	MPIAFGQVRARPIPKEKEKGRLG-----ENRAETBQEVILLGDAVQCRVCYERVQDKEDS	
fishSLX1	146	IPLIFGQCRAKRKP-----OIVSKQD-----ERQVELCVLCGEFIKTVR	
flySLX1	175	MDIVSKVVISASQ-----RQRTDABVPPP--VAWASECHLQMQLIQPERSR-----	
wormSLX1	313	TKRECKWKKEMSLVP-----SREDYLMG-----ECRICKDILKLWSL	
pombeSLX1	143	INYFDEEWLNGFHE-----VIQKTYDHKLCLRKTISEPVICNLQYECIISDPLR	
Slx1p	158	INQINENALEEPKEITVDVLMHDHSDENLKVVEAVYTKVIENERNIFTEKKLLTGVVICFCCEKEIYTSEEQNLKPF	
consensus	321	vpl fg v r r e e rC lCa ie e	
humanSLX1	200	-LCPHPGLPRAHVICLAAEFLQDE----PGDLPPIEGCCPCCEKSLLWGDLIWLCQ---MDKEVVESETEEAHW	
mouseSLX1	196	-LCPHPGLPRAHVIICLAAEFLQDE----PGDLPPIEGCCPCCEKSLLWGDLIWGCQ---ADPEEE-EPLEEEPHW	
frogSLX1	205	-LCPHPGLPRAHVIICLAAEFLQDE----PGDLPPIEGCCPCCEKSLLWGDLIRHRNG--CYCDLEEIS--SSQAHW	
fishSLX1	187	-LCPHPHSQIVCHLICLAAEFLQDE----PGDLPPIEGCCPCCEKSLLWGDLILYKN---ADLEEMNIPSSQNHW	
flySLX1	222	-LCPTNQMRPCTHMMCLANYLQDE----PGHLYIPVNGCCPCCEKSLLWGDLIQRKRLLLGVPKEDYEDIEDID	
wormSLX1	354	-MPCISATPSHPSKCLSENCLKLKN--EVHDHYPKIANCPCTCGOFYLGWDIIRBQRRRIKISKCAEEFONIVVRKE	
pombeSLX1	194	-ANCPFTDINSNHTCLASSPLDE----CQVLPTEGCTCKEVPRPREFSTVFT----SLETRPFESENR	
Slx1p	238	VALCNNKDHGCVNHIKCLHYPLDDEQLMVGRNLIPRGGSQPCCDMFCIDWTIVFKFSTR-----MKLAG	
consensus	401	l C hp C l HviCl a fL ee p qliPleg C p C ksllWgdl teleeed el hw	
humanSLX1	270	TDLT-----	
mouseSLX1	265	TDLT-----	
frogSLX1	274	GHRCS-----	
fishSLX1	255	TDLQL-----	
flySLX1	296	VSNIEDTP-----	
wormSLX1	431	LPHREISPISSKK	
pombeSLX1	262	IBIHDLELEK---	
Slx1p	304	K-----	
consensus	481	d le	

Figure S4. Multi-sequence alignments of eukaryotic C20orf94-related proteins. Sequences were analyzed using CLUSTALW and displayed using BOXSHADE.

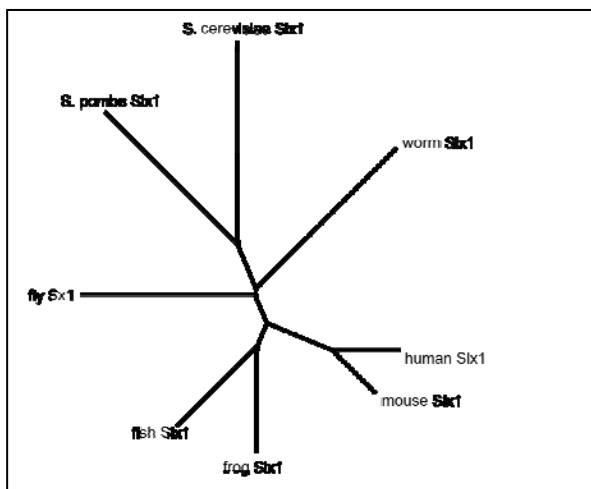
ratC20orf94	1	MASKKFVIKCGNFAVLVDLHVLPOGSNKDSWFWSEQKKEEVCLLLKETIDS RVKEYVGYKQH-RPSIA-EFSRSSPLSLKGYGFQITAY
mouseC20orf94	1	MASKKFAVKCGNFAVLVDLHVLPOGSNRDSSWFSEQKKEEVCLLLKETIDS RVKEYVGYKQH-KPSIA-EFRSSPLSLKGYGFQITAY
humanC20orf94	1	MASKKFAVKCGNFAVLVDLHILPOGSNKDTSWFSEQKKEEVCLLLKETIDS RVKEYVGYKQH-RPSNA-EFRSNPLSLKGYGFQITAY
chickenC20orf94	1	MASKKFVIKCGNFAVLVDLHILPOGSNKDTSWFSEQKKEEVCLLLKETIDS RVKEYVGYKQH-EHASSSLFVTNNFHITAY
frogC20orf94	1	--MVKLVVKCGNFAVLVDLQVLPQGTSKDTSWFSEQKKEEVCLLEEVWSR LKHYPQKQSM-EHASSSSLFVTNNFHITAY
fishC20orf94	1	MEPSKFVVKGNYAVLVDLHIALGDODNANWFSPAHEKEVGSLIRDALEPR VRQFOEARYOIQSKPRKDUTPTAPICL EGNVRUA VH
consensus	1	maskKfvvKCGNFAVLVDLhvLpqGsnkdtswFSeqkkeEVclllketids RvkeyleirkQh qp ta efrssPLslkgygfqtay
ratC20orf94	89	FIRRGIHLRCIQSFRNTELRIFPESFVVCVSQLAFGHDIWANONEKSTQR-ALHGA SDYFAOCAES---SPPDGIKLKRNTLKEIVRRAE
mouseC20orf94	89	FLKRGRIHLPCIQNSQNTIELRVFPERFVVVCVSQLAFGHDIWANONEKSTKK-ALHGV SDYFPECAES---SPSEGTTKLKRNTALKEIVRRTK
humanC20orf94	89	FLKRGIRLRCIRSCTQAEIQLVRFVFPERFVVVCVSQLAFGHDIWANONEKSTKK-SLPESAKLRNALKEIVRRTK
chickenC20orf94	90	FMKEWVNLRQALGKHYRELRFMPDKFVVVLSKTEENPASAWTCEN-GALKE-VSNGT SYFAE SAENRKLKLSLNEQI KQDILKEMTKKGK
frogC20orf94	88	FIKRWVKLRCVVKRQHYRELRFVFPERFVVVCASQLEPASSTWVTEAAA D KESCSGGTSYFAQPKGIE-MTNLLTTPAQAVALKNIVRRTK
fishC20orf94	91	FMKRHVNLRCIVRQHYRELRFVFPERFVVVCASPPENSALPNGLNDVSEQ---SQERYFSNSCTAN-PLOSSSTATKRAVIIQKIAKRTK
consensus	91	FikRgihLrCil sq rELrvFPerfVV CvSql fghdiwanqe stkr lhg SdYfaecaes sl p tkkrnilkeivrrtk
ratC20orf94	175	SKGIDVSKPQTSD-----LVGSSSDSVITVTPWRRD-----ASAIIILSE-----PVGQAQDDIRAAKSHQ
mouseC20orf94	175	SKGIDVSKPQPSED-----LVGSSSDSVITVTPWRRD-----ASAIIILSE-----SVGQAQDDIRAAKSHQ
humanC20orf94	175	TKSSVTTSKSCTRRD-----TVESSSDSVIAELIARRRN DG-----QASSSPSE-----SMGOAKDSIKAAESHW
chickenC20orf94	4178	NS--VSKPQTSD-----SKKVDLGSIGSQTCGNRND C-----Q1SPGPQSEVKWRSTGRLLKNCINTAESNL
frogC20orf94	176	IT-KDISDEAERDS-----RVSFSLGLADTGKEDANNIQ-----KALSQAQPE-----EKREEPNDYINTDSL
fishC20orf94	176	IQPPRSQDNESKGTGQFQADNAEGSRSVLRQANIQPQQCQDDQVYKSGQFQADKQEK-SGGDVLUQKITRQANI PQQCQDDQESKS
consensus	181	sk tdkvskpqtsrd v kssdsvit varrrn asa llse svgqaqddiraaesh
ratC20orf94	231	ELPVQKLEN-----VSQTQPGDTRSSQQLHPGEWLKTGLLSRSPVYNYESASPGPKQS PRAAKTQQKRR-----
mouseC20orf94	231	ELPVQKLEN-----VSQTQPGDTRSSQQLHPGEWLKTGLLSRSPVYNYESASPGPKQS PRAAKTQQKRR-----
humanC20orf94	234	GLPVQKLEK-----VNQTQPGDTSQGQKPHPGERLKTGLLSRSPVCSCEASPCPKQSPRVAKTQQKRR-----
chickenC20orf94	4238	EFPVLELENN-----VNQROPEDASSQKPHFVEOLKSRLLSKNSPCSYEASALLGPKNQKETETQAAQK-----
frogC20orf94	235	GLPVPEVEND-----VNHRQPSBASSQKPKQ-CAELKTTQDLSKHLSRLSDSAK-QTOSLRASVMQOKRR-----
fishC20orf94	266	GQVQADKENGSGDVLHKIAKQIN TQPPQSQDQEFKS QOF PAGESEKGSRSVLUQEPKQANIQSPHSQED-BFKSGQFQVAEECVAACL
consensus	271	lpvqklen vnqtQP dtssqQkphpgewlktgllsrsp yesAspgpkQspraktQkrr
ratC20orf94	295	-----NCGSVEDSDHRRRVSLGNEGLVPEDSVVETSTAVRVLPALELSPG-----LLLKDQDLAKATAKEELHALENLSSRHLVT----D
mouseC20orf94	295	-----NCGSVEDCDHRRRVSLGNEGLVPEDADRERSTAVRVLPALELSPG-----LLLKDQDLAKAKAKEELHALENLSSRHLVT----N
humanC20orf94	298	-----NCSSAEDFDHICRVSLSGSDRLVPRERIIVEKSKAVRVLPASELSPDG-----LLLKDQDLAKTTSKEELHVLESLSRRHLMK----N
chickenC20orf94	4303	-----SCSSEEKLDFKIEISSEEAPELPSNTERSKCSDDHGLFLEKTPLNSRIFSKQDITEIASDEELITFGKNLSPRIPMRTNQN
frogC20orf94	297	-----RHSS-EGKERCKKSCITSDFTQQGMQRNE-AQVKDLEHVP--LASQTIPVRHVSADRGDTLPKPAAI-SV-----
fishC20orf94	356	PVPISVSSSIKSLVVKALSSSKSNKDTESYDTTGPRRPRAPSSSGEDDHQKTKRLRQSAVSSDSNNPSSGIAAPDSVCSPOP
consensus	361	ncsSved dhrrrvslgne lvped vrerstavrvlpalelsdp g lllkqdlak skeelh leslssrhlm n
ratC20orf94	371	NPGQARPTCSATVTERLAPVQSGPS-----KKRKKIQSSSRGCGSGKKS-----
mouseC20orf94	371	NPGQAQOSDSSAAITEQLADQGEGPS-----KKRKKIQSYNRGCGSGKKN-----
humanC20orf94	374	NPGQAQOQIGLATINTERLSTIONSP-----KKRKK--YERGH-----
chickenC20orf94	4386	EPGTAATEELPVVPSSSYLEMQAVSSEQL--IQKRKKEGEDGLRKLKLRLKKP
frogC20orf94	365	--ASKQQQCALSFNSIHTEQSVKAVLA--PLLNKDP-----
fishC20orf94	446	EISQTNOQCLATSLRGLSVKPVSSGSSISSRPAAERKGGEPRTSRLRLKKK
consensus	451	npgqaaqtg atvte l tvq ps kkrkk l rg s k

Figure S5. Phylogenetic trees for eukaryotic SLX4, SLX1, and C20orf94. CLUSTALW tree files were used to generate trees in TREEVIEW. A, SLX4; B, SLX1; C, C20orf94.

A. SLX4



B. SLX1



C. C20orf94

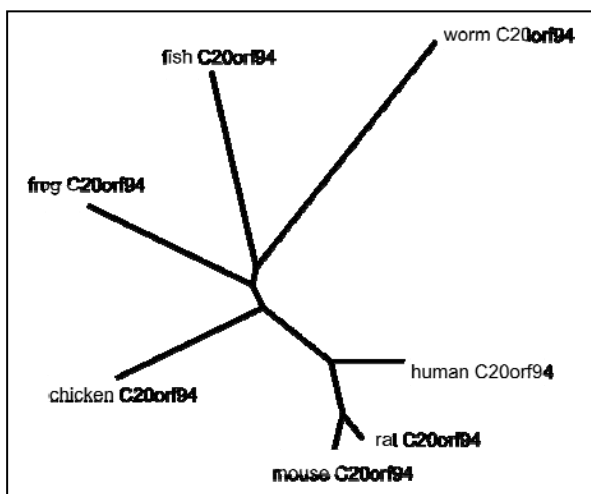


Figure S6.

Interaction of PLK1 with SLX4. (A)
Consensus polo-box binding site defined by

SCANSITE (mit.scansite.edu) and the sequence of a candidate polo-box binding site in human SLX4 wherein S1453 is a candidate phosphoserine. (B) PLK1 interacts with SLX4 in the two-hybrid system but not with SLX4 in which S1453 is replaced by alanine. As a control, SLX4^{S1453A} was shown to maintain the interaction with SLX1. (C) Mutation of S1453 to alanine in SLX4 reduces the interaction with PLK1 in 293T cells. Cells expressing either Myc-SLX4 or Myc-SLX4 Δ N (residues 684-1835) with or without the S1453A mutation were lysed and immunoprecipitated with anti-Myc antibodies. Immunoblots were probed with either anti-PLK1 to detect endogenous PLK1 or anti-MYC to detect SLX4. (D) PLK1 phosphorylates SLX4 *in vitro*. Extracts from cells expressing MYC-SLX4 were subjected to immunoprecipitation with anti-MYC antibodies and *in situ* phosphorylation assays performed by addition of γ^{32} P-ATP. Products were examined by SDS-PAGE and autoradiography to detect phosphorylation or by immunoblotting to detect MYC-SLX4. To examine whether PLK1 was responsible for SLX4 phosphorylation, *in vitro* assays were supplemented with a small molecule inhibitor of PLK1 (BI2536, 100 nM), which dramatically reduced SLX4 phosphorylation. (E) PLK1 interacts with ERCC4 via SLX4. Cells expressing HA-PLK1 were transfected with a control (CK) siRNA or 2 siRNAs targeting SLX4 and extracts subjected to anti-HA IPs and immunoblotting. Depletion of SLX4 reduced the levels of ERCC4 associated with PLK1.

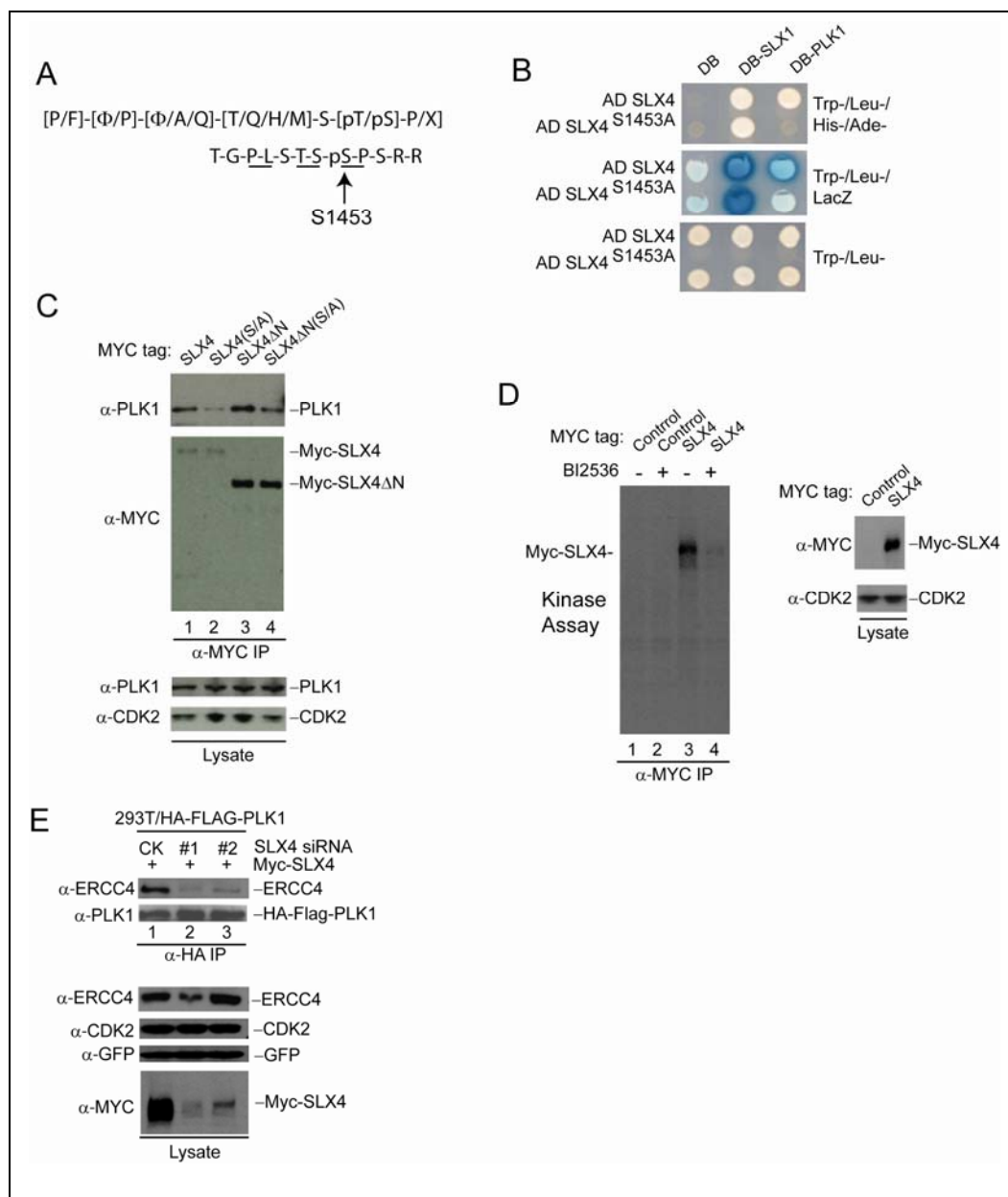


Figure S7. Co-localization of TERF2IP (RAP1) with GFP-SLX4. HeLa cells with long telomeres (from Jan Karlseder, the Salk Institute) were transiently infected with a lentivirus expressing GFP-SLX4 and after 48 hours, cells were permeabilized, fixed and stained with anti-TERF2IP using Alexa fluor 594-conjugated secondary antibodies. Cells were imaged using a confocal microscope. Representative examples of cells expressing GFP-SLX4 are shown.

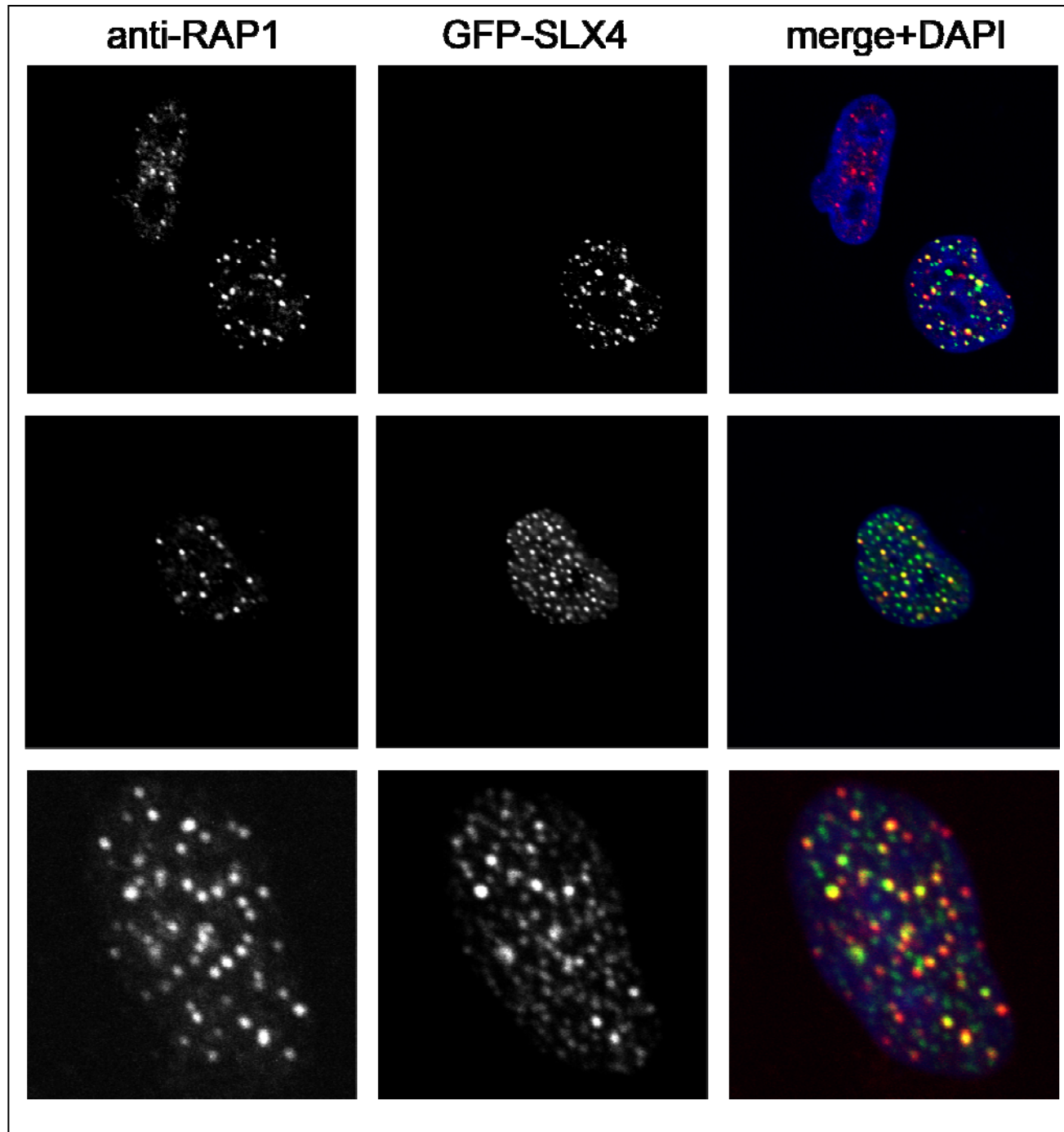


Figure S8. Co-localization of ERCC4 and MUS81 with GFP-SLX4. U2OS cells were transiently infected with a lentivirus expressing GFP-SLX4 and after 48 hours, cells were permeabilized, fixed and stained with either anti-ERCC4 (panel A) or anti-MUS81 (panel B) using Alexa fluor 594-conjugated secondary antibodies. Cells were imaged using a confocal microscope.

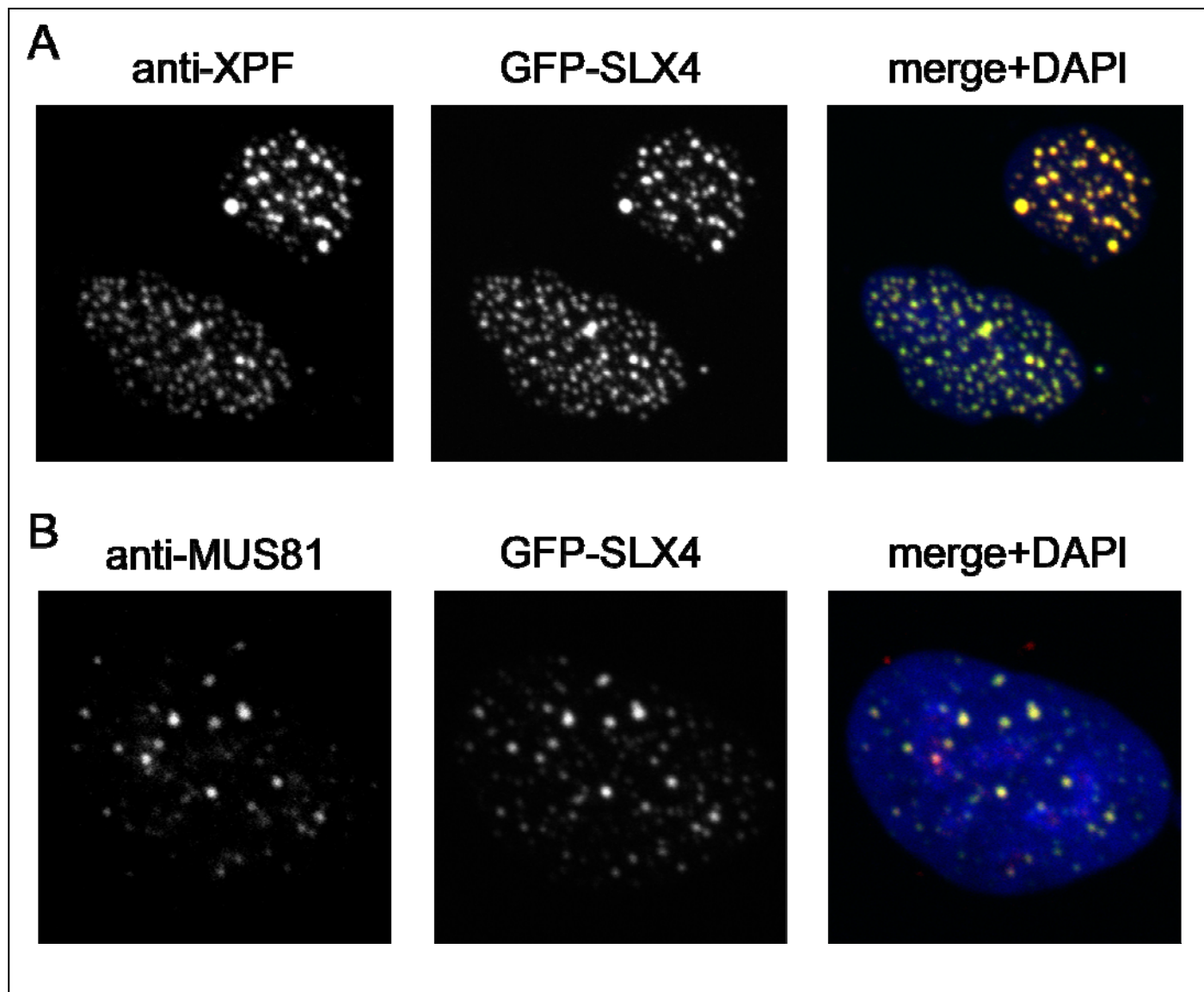


Figure S9. qPCR analysis of cells depleted of SLX1, SLX4, or GEN1 by RNAi. HeLa cells were reverse transfected with the indicated siRNAs as described in the Supplemental Experimental Procedures. After 72 h, total RNA was isolated and subjected to reverse transcription prior to quantitative PCR using gene-specific primers. Quantitative PCR was performed on a LightCycler 480 (Roche) using GAPDH as an internal control.

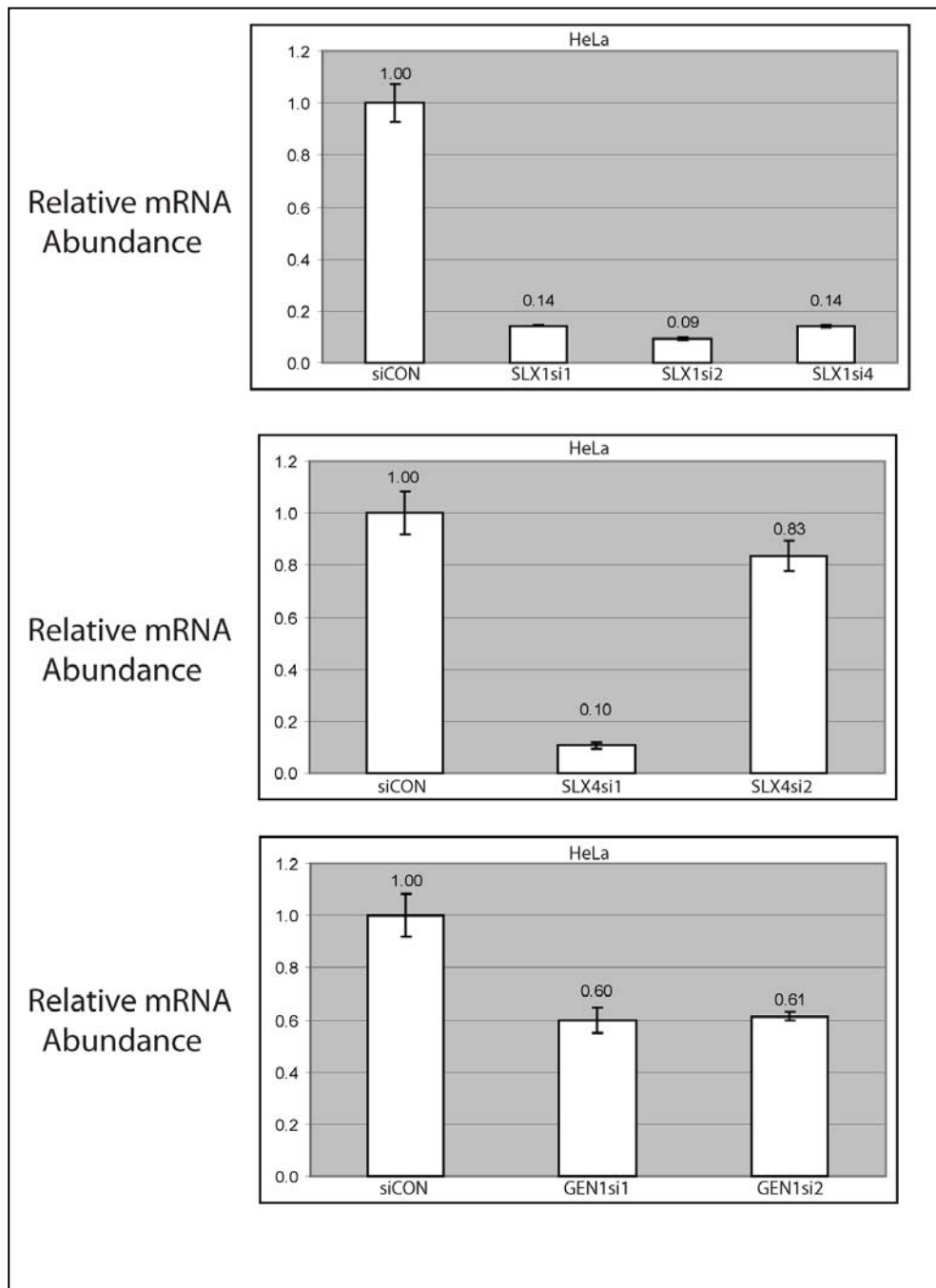


Figure S10. Structures of the Holliday junction (X0) substrates used in this study. Substrates were labeled on either strand 1 or strand 3 as indicated (*).

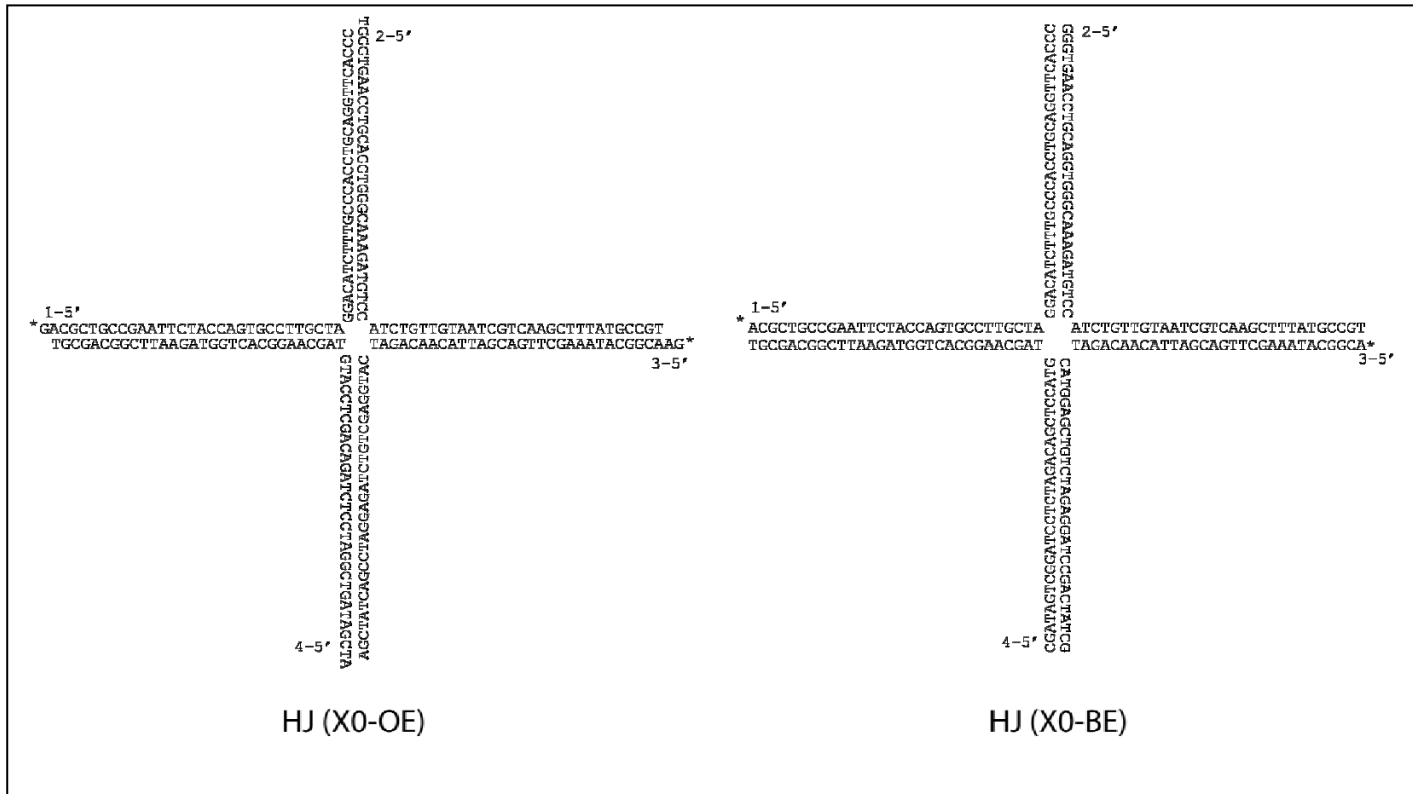


Figure S11. Reproducibility of SLX4 complex analysis by mass spectrometry. SLX4 immune complexes were prepared without (SLX4UT and iSLX4) or with treatment of cells with CPT (SLX4+CPT) or MMC (SLX4+MMC) (8 h) and cell extracts processed for immunoprecipitation and LC-MS/MS. TSCs for interacting proteins validated in this study are shown. All SLX4 constructs were C-terminal HA fusion proteins; iSLX4 is a tet-inducible version of SLX4. GIYD2=SLX1.

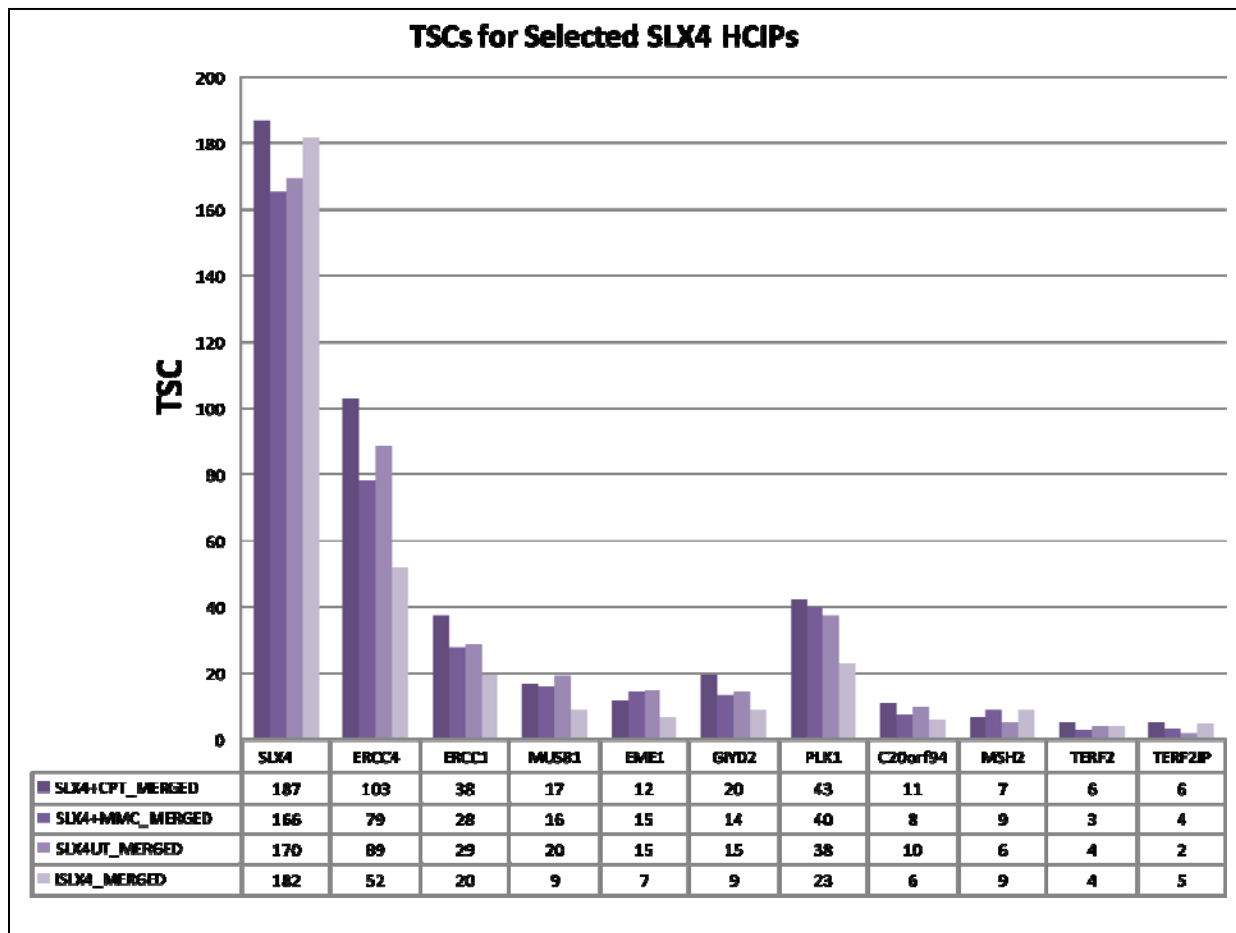


Figure S12. Comparison of MUS81-HA and SLX4-HA activity toward static Holiday junctions (panel A) at equivalent amounts of MUS81 protein. Extracts from 293T cells expressing either MUS81-HA (50 µg) (lanes 1 and 2 in Panel B) or SLX4-HA (500 µg) (lanes 3 and 4 in Panel B) were subjected to immunoprecipitation with anti-HA antibodies such that the resulting complexes contained identical levels of MUS81 protein, as assessed by immunoblotting (lanes 1 and 2 in Panel D). These complexes were then used for cleavage assays with HJ (X0-OE) and the products separated on denaturing gels (Panel B). While robust largely symmetrical cleavage was observed with SLX4-HA complexes (lanes 3 and 4 in Panel B), no cleavage was observed with MUS81-HA complexes under these conditions (lanes 1 and 2 in Panel B). In contrast, when a much larger amount of the MUS81-HA lysate (500 µg) was employed for immunoprecipitation and the products analyzed on native gels, significant 3'-flap, replication fork and HJ (X0-OE) activity was observed (Panel C, lanes 5-7), indicating that the MUS81-HA protein was catalytically active in this setting. Immune complexes were immunoblotted for MUS81 (Panel D) to demonstrate the relative levels of MUS81 present in each of these immune complexes. Arrows in Panel A indicate sites of cleavage in the X0-OE substrate. (Panel E) Extracts from 293T cells were immunoprecipitated with anti-SLX4^C or with control IgG sequentially 3-4 times and the immune complex and lysate (5% of input) immunoblotted using anti-SLX4^M, anti-ERCC4, and anti-MUS81 antibodies. The asterisk indicated the position of a non-specific band present in the control and anti-SLX4 IPs that co-migrates with MUS81. Only a small portion of MUS81 is depleted from extracts, indicating that the majority is not associated with SLX4.

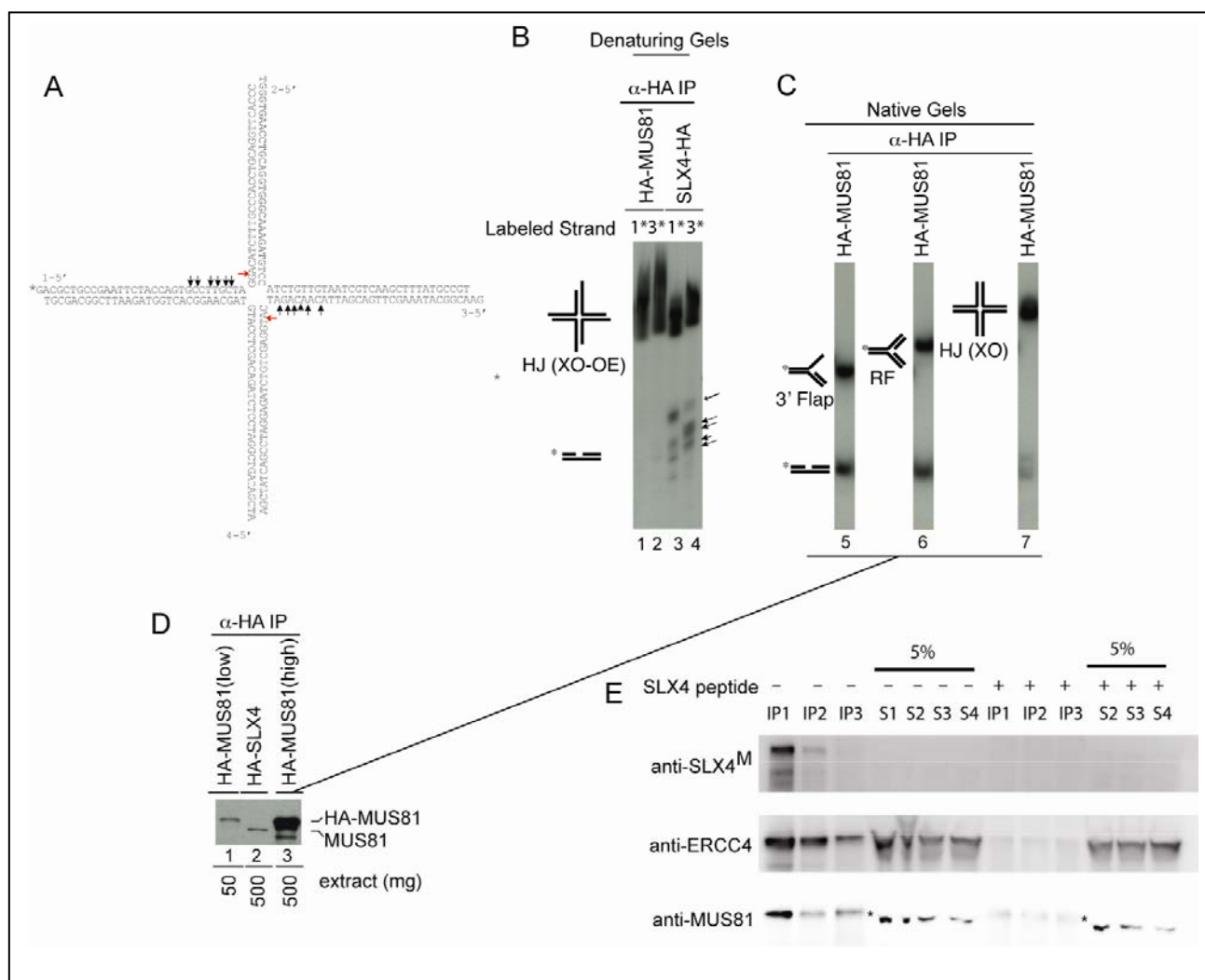


Figure S13. Depletion of SLX4 in U2OS cells leads to sensitivity to DNA damage agents. (A, C, D) The indicated shRNAs were infected into U2OS cells and MCA assays performed as described under Experimental Procedures. ATM and ATR shRNAs were employed as positive controls. (B) Cells used in (A) were analyzed by IP-WB for expression of SLX4. (E, F) U2OS cells transfected with the indicated siRNAs were subjected to MCA assays (E) or quantitative PCR (F)

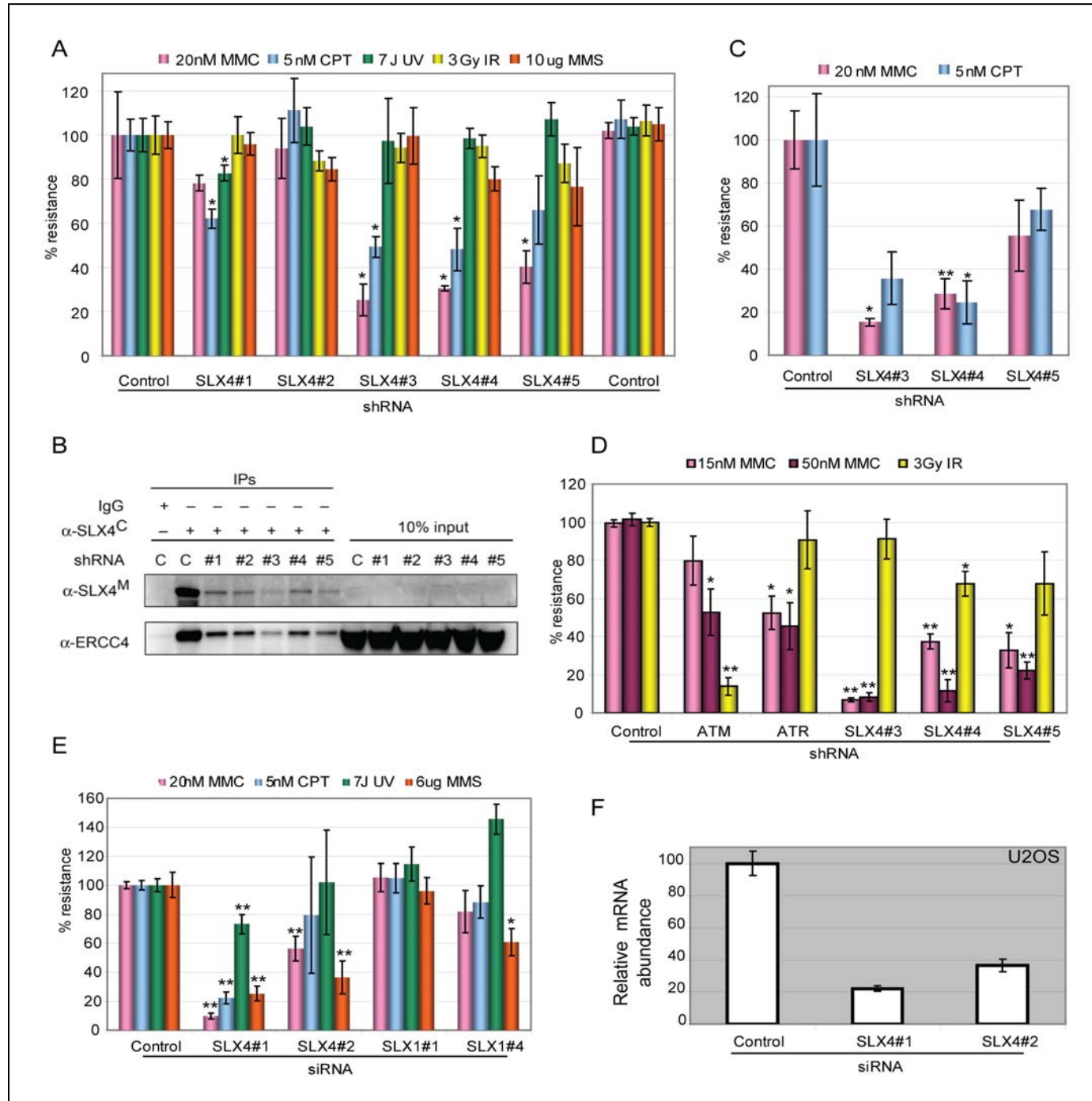


Figure S14. Regions of SLX4 sufficient for MUS81 binding. 293T cells transiently expressing the indicated MYC-tagged SLX4 fragments (panel A) were lysed and subjected to immunoprecipitation with anti-MYC. Immune complexes and lysates were subjected to immunoblotting (panel B). The region of SLX4 encompassing amino acids 1328-1648 was sufficient to interact with MUS81 (lane 3).

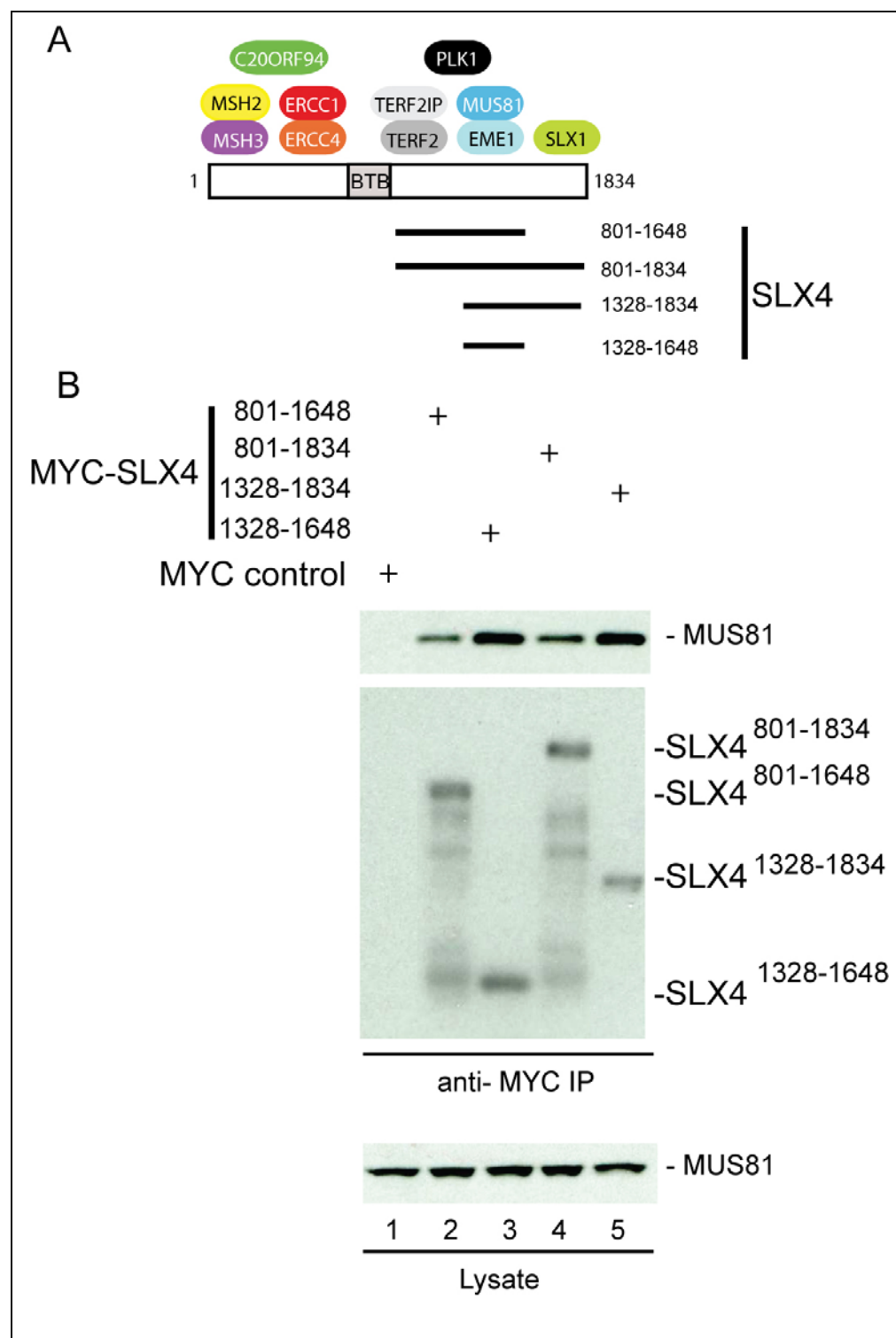


Figure S15. Recombinant GST-SLX1/His₆-SLX4-C displays activity toward a 5'-Flap substrate. GST-SLX1/His₆-SLX4SBD (3 ng) purified from bacteria was incubated with a radiolabeled 5'-flap substrate (30 min, 30°C) and the products analyzed on a native gel. The catalytically defective (CD) GST-SLX1^{E82A} mutant did not display this activity.

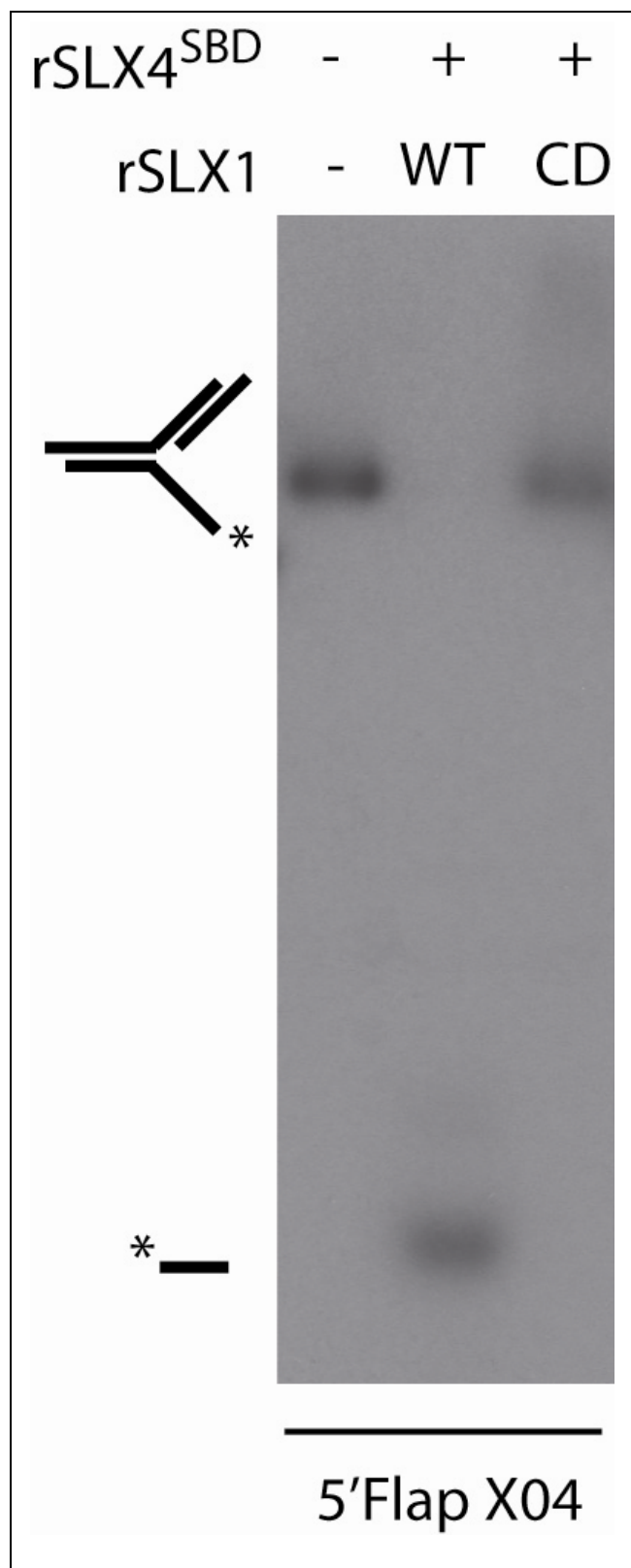


Figure S16. Cell cycle profiles of U2OS cells expressing shRNAs targeting SLX4. Cells were infected with lentiviruses expressing the indicated SLX4 shRNAs and 5 days later, cells were analyzed for cell cycle distributions after propidium iodide staining.

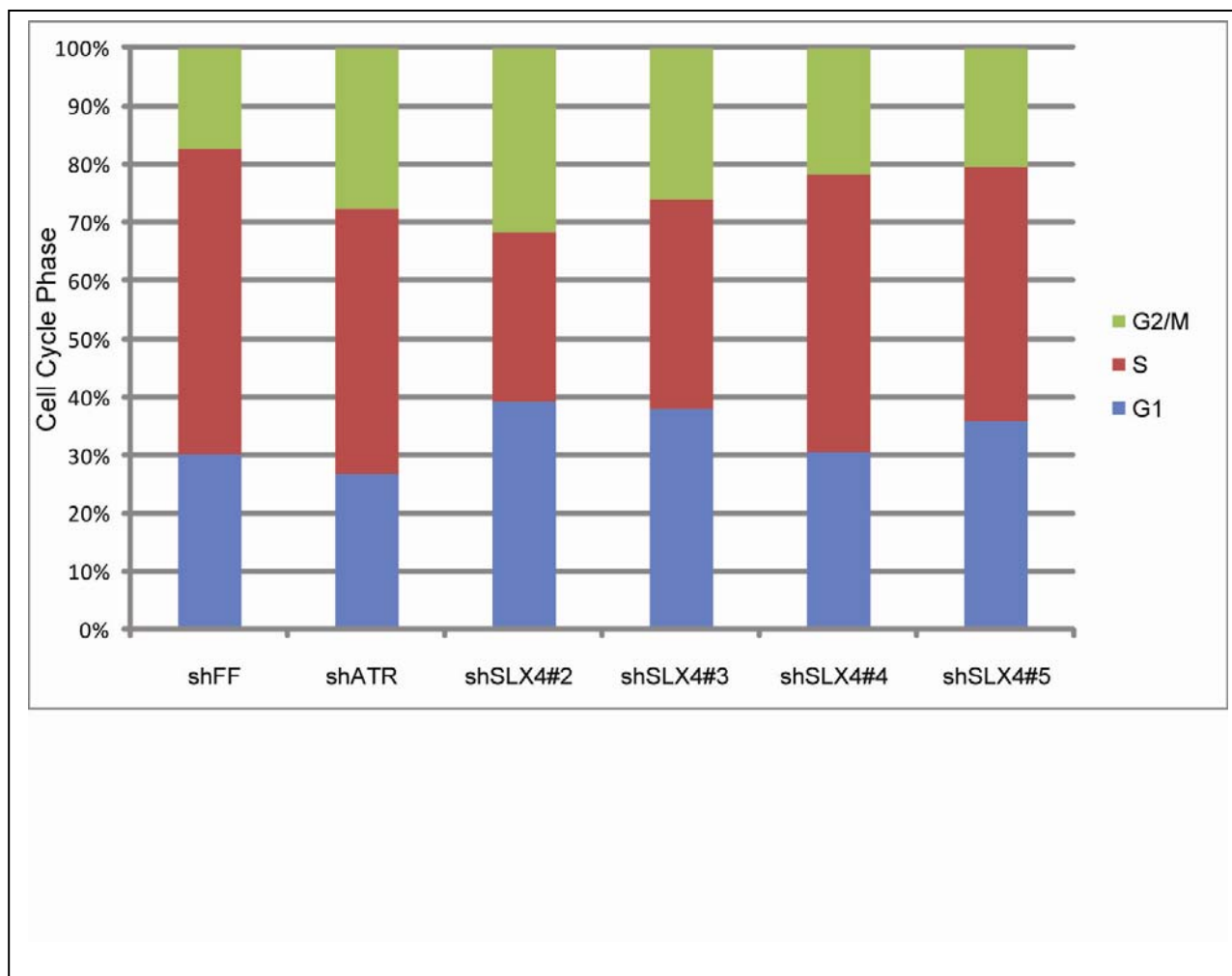
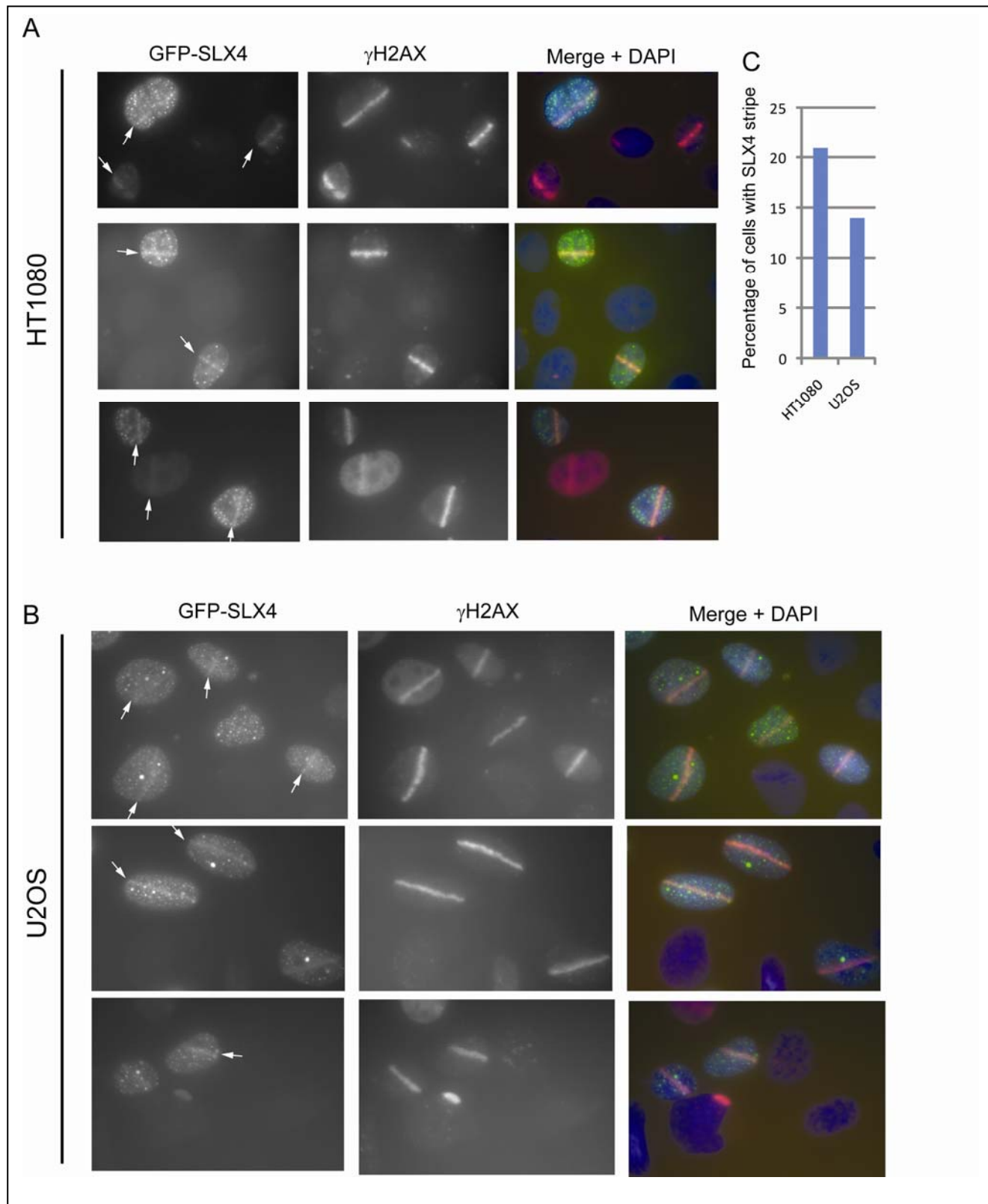


Figure S17. Localization of GFP-SLX4 to sites of laser microirradiated DNA damage. (A) Images of HT1080 cells transiently expressing GFP-SLX4 30 min after microirradiation. Sites of DNA damage are indicated by staining with γ H2AX. (B) Images of U2OS cells transiently expressing GFP-SLX4 30 min after microirradiation. Sites of DNA damage are indicated by staining with γ H2AX. (C) Quantification of cells in which GFP-SLX4 co-localized with the γ H2AX in a stripe. n = >300 irradiated cells.



Supplemental References

- Bekker-Jensen, S., Lukas, C., Kitagawa, R., Melander, F., Kastan, M. B., Bartek, J., and Lukas, J. (2006). Spatial organization of the mammalian genome surveillance machinery in response to DNA strand breaks. *J Cell Biol* 173, 195-206.
- Ciccia, A., Constantinou, A., and West, S. C. (2003). Identification and characterization of the human mus81-eme1 endonuclease. *J Biol Chem* 278, 25172-25178.
- Ip, S. C., Rass, U., Blanco, M. G., Flynn, H. R., Skehel, J. M., and West, S. C. (2008). Identification of Holliday junction resolvases from humans and yeast. *Nature* 456, 357-361.
- Rass, U., and West, S. C. (2006). Synthetic junctions as tools to identify and characterize Holliday junction resolvases. *Methods Enzymol* 408, 485-501.
- Smogorzewska, A., Matsuoka, S., Vinciguerra, P., McDonald, E. R., 3rd, Hurov, K. E., Luo, J., Ballif, B. A., Gygi, S. P., Hofmann, K., D'Andrea, A. D., and Elledge, S. J. (2007). Identification of the FANCI protein, a monoubiquitinated FANCD2 paralog required for DNA repair. *Cell* 129, 289-301.
- Sowa, M. E., Bennett, E., Gygi, S.P. and Harper, J.W. (2009). Defining the human deubiquitinating enzyme interaction landscape. *Cell*, *in press*.
- Xia, B., Sheng, Q., Nakanishi, K., Ohashi, A., Wu, J., Christ, N., Liu, X., Jasins, M., Couch, F. J., and Livingston, D. M. (2006). Control of BRCA2 cellular and clinical functions by a nuclear partner, PALB2. *Mol Cell* 22, 719-729.
- Xu, L., Sowa, M. E., Chen, J., Li, X., Gygi, S. P., and Harper, J. W. (2008). An FTS/Hook/p107(FHIP) complex interacts with and promotes endosomal clustering by the homotypic vacuolar protein sorting complex. *Mol Biol Cell* 19, 5059-5071.